

# Grand canonical steady-state simulation of nucleation

Martin Horsch and Jadran Vrabec\*

*Universität Paderborn, Lehrstuhl für Thermodynamik und Energietechnik,  
Warburger Str. 100, 33098 Paderborn, Germany*

(Dated: October 16, 2009)

## Abstract

Grand canonical molecular dynamics (GCMD) is applied to the nucleation process in a metastable phase near the spinodal, where nucleation occurs almost instantaneously and is limited to a very short time interval. With a variant of Maxwell's demon, proposed by McDonald [Am. J. Phys. 31 (1963): 31], all nuclei exceeding a specified size are removed. In such a steady-state simulation, the nucleation process is sampled over an arbitrary timespan and all properties of the metastable state, including the nucleation rate, can be obtained with an increased precision. As an example, a series of GCMD simulations with McDonald's demon is carried out for homogeneous vapor to liquid nucleation of the truncated-shifted Lennard-Jones (tsLJ) fluid, covering the entire relevant temperature range. The results are in agreement with direct non-equilibrium MD simulation in the canonical ensemble. It is confirmed for supersaturated vapors of the tsLJ fluid that the classical nucleation theory underpredicts the nucleation rate by two orders of magnitude.

---

\* Corresponding author. Email: jadran.vrabec@upb.de

## I. INTRODUCTION

The key properties of nucleation processes are the height  $\Delta\Omega^*$  of the free energy barrier that must be overcome to form stable embryos of the emerging phase and the nucleation rate  $\mathcal{J}$  that indicates how many nuclei appear in a given volume per time. The most widespread approach for calculating these quantities is the classical nucleation theory (CNT)<sup>1</sup>, which has significant shortcomings, e.g., it can overestimate  $\Delta\Omega^*$  significantly for homogeneous vapor to liquid nucleation<sup>2</sup>. A more accurate theory of homogeneous nucleation, which is sought after, would also increase the reliability for more complex applications such as heterogeneous and ion-induced nucleation in the earth's atmosphere.

An important problem of CNT is that the underlying basic assumptions do not apply to nanoscopic nuclei<sup>3</sup>. Although it is possible to measure the critical size by neutron scattering<sup>4,5</sup>, the thermophysical properties of such nuclei are mostly very hard to investigate experimentally. However, they are well accessible by calculations based on density functional theory<sup>6-9</sup> as well as molecular simulation<sup>10-12</sup>. For instance, vaporization processes<sup>11</sup> and equilibria<sup>10,12</sup> of single liquid droplets can be simulated to obtain the surface tension as well as heat and mass transfer properties of strongly curved interfaces. Similarly, very fast nucleation processes that occur in the immediate vicinity of the spinodal are experimentally inaccessible, whereas they can be studied by Monte Carlo (MC)<sup>13</sup> and molecular dynamics (MD)<sup>14,15</sup> simulation of systems with a large number of particles. Lower nucleation rates are accessible by transition path sampling based methods such as forward flux sampling<sup>16,17</sup>. Hence, molecular simulation is crucial for the further development of nucleation theory.

Such MD simulations, dealing with single nuclei in equilibrium as well as with homogeneous nucleation processes in supersaturated vapors, led to the formulation of a surface property corrected (SPC) modification of CNT for vapor to liquid nucleation of unpolar fluids, cf. previous work<sup>15</sup> for a detailed presentation and justification. Both CNT and the SPC modification apply the expression

$$\left(\frac{\partial\Omega}{\partial\nu}\right)_{\mu,V,T} = \gamma \left(\frac{\partial\mathcal{F}}{\partial\nu}\right)_{\mu,V,T} - [\mu - \mu_\sigma(T)], \quad (1)$$

accounting for the positive contribution of the surface tension  $\gamma$  acting on the surface area  $\mathcal{F}$  as well as a negative bulk contribution, where  $\mu$  and  $\mu_\sigma(T)$  are the chemical potential of the supersaturated and the saturated vapor at the temperature  $T$ , respectively, to the free

energy of formation

$$\Delta\Omega_\nu = \int_1^\nu \left( \frac{\partial\Omega}{\partial\nu} \right)_{\mu, V, T} d\nu, \quad (2)$$

for a nucleus containing  $\nu$  particles. The maximal free energy of formation  $\Delta\Omega^*$ , corresponding to the critical size  $\nu^*$ , is the decisive quantity for the nucleation rate, given by the Arrhenius equation as

$$\mathcal{J} = A \exp\left(\frac{-\Delta\Omega^*}{k_B T}\right), \quad (3)$$

where  $k_B$  is the Boltzmann constant. In addition to the usual collision term from kinetic gas theory, the pre-exponential coefficient  $A$  includes the Zél'dovič (Зельдович) factor and a correction for thermal non-accomodation<sup>1</sup>. Although  $A$  is not constant, it depends to a much lower extent on supersaturation than the exponential term. CNT applies the capillarity approximation, which in the present context means that  $\gamma$  is assumed to be the same as the surface tension of the planar vapor-liquid interface  $\gamma_\infty$ . The surface area is determined from the assumption that all nuclei are spherical. The SPC modification replaces the capillarity approximation with the Tolman equation<sup>18</sup>,

$$\frac{\gamma_\infty}{\gamma} = 1 + \frac{2\delta}{\mathcal{R}}, \quad (4)$$

wherein  $\mathcal{R}$  is the radius of the nucleus and  $\delta$  is the Tolman length, a characteristic interface thickness, while the surface area is increased by a steric factor  $s$ . In particular, the temperature-dependent correlations

$$\delta/\mathcal{R} = \left( \frac{0.7}{1 - T/T_c} - 0.9 \right) \nu^{-1/3}, \quad (5)$$

with respect to the critical temperature  $T_c$ , as well as

$$s = \frac{0.85(1 - T/T_c)^{-1} + (\nu/75)^{1/3}}{1 + (\nu/75)^{1/3}}, \quad (6)$$

can be used for unpolar fluids<sup>15</sup>. A different approach is given by the Hale<sup>19</sup> scaling law (HSL). In agreement with experimental data on nucleation of water and toluene<sup>19</sup>, it predicts

$$\mathcal{J} \sim \rho^{-2/3} \left( \frac{\gamma_\infty}{T} \right)^{1/2} p^2 \exp\left(\frac{4(k_B T)^2 \gamma_\infty^3}{27(\mu - \mu_\sigma)^2}\right), \quad (7)$$

where the proportionality constant only depends on properties of the critical point.

The present work has the objective of refining the methodology used for direct MD simulation of nucleation processes. According to the method of Yasuoka and Matsumoto<sup>14</sup>

(YM), a supersaturated vapor is simulated in the canonical ensemble and the nucleation rate is obtained from the number of nuclei formed over time, using a linear fit where only nuclei that exceed a sufficiently large threshold size are counted. Nucleation occurs after the metastable state is equilibrated and before nucleus growth becomes dominant. However, the timespan corresponding to nucleation is very short for the high nucleation rates that are accessible to direct MD simulation, which restricts the statistical basis and the precision of the results. Near the spinodal, the regimes of equilibration, nucleation, and growth even start to overlap and the YM method becomes unreliable.

Wedekind *et al.*<sup>20</sup> recently developed a more rigorous method which is based on mean first passage times (MFPT) obtained by averaging over hundreds of simulation runs. But as Chkonia *et al.*<sup>21</sup> point out, ‘the computational costs of making the necessary repetitions to evaluate the MFPT can be very high,’ whereas ‘YM requires many clusters forming and it therefore becomes more sensible to deviations coming from vapor depletion or coalescence of clusters.’

A new direct equilibrium MD simulation method is introduced in the present work. The underlying concept is to simulate the non-equilibrium as a stationary process in the grand canonical ensemble. Thereby, it is possible to sample exclusively nucleation as opposed to nucleus growth and coalescence. While the precision of the results is increased by maintaining the steady state over an arbitrarily long time interval, the advantages of the YM non-equilibrium method are also retained. In particular, only one MD simulation run is required and the nucleation rate is obtained from the number of large nuclei formed over time. This is achieved by combining grand canonical molecular dynamics (GCMD), introduced by Cielinski<sup>22</sup>, and an ‘intelligent being’ that continuously removes all large nuclei: McDonald’s demon<sup>23</sup>.

## II. SIMULATION METHOD

In a closed system, nucleation is an instationary process because the metastable phase is depleted by the emerging nuclei. The idea behind the present approach is to simulate the production of nuclei up to a given size for a specified metastable state. Nuclei above the given size are extracted, and particles are inserted as monomers into the system to replenish the metastable phase.

GCMD regulates the chemical potential and samples the grand canonical ensemble: alternating with standard MD steps, particles are deleted from and inserted into the system probabilistically with the usual grand canonical acceptance criteria<sup>22,24</sup>. For a test deletion, a random particle is removed. For a test insertion, the coordinates of an additional particle are chosen at random. The potential energy difference  $\delta\mathcal{V}$  is determined for each of the test operations and compared with the residual chemical potential. The acceptance probability is defined the same way as for the Metropolis algorithm, i.e., it is

$$P = \min \left( \rho \Lambda^3 \exp \left[ \frac{-\mu - \delta\mathcal{V}}{k_B T} \right], 1 \right), \quad (8)$$

in case of deletions and similar for insertions<sup>25</sup>. In this expression,  $\rho$  is the density and  $\Lambda$  is the thermal wavelength. The number of test deletions and insertions per simulation time step was chosen in this work between  $10^{-6}$  and  $10^{-3}$  times the number of particles.

Whenever a nucleus exceeds the specified threshold size  $\Theta$ , McDonald's demon<sup>23</sup> – called Szilárd's demon by Schmelzer *et al.*<sup>26</sup> – removes it from the system and replaces it by a representative configuration of the metastable phase. If a dense phase is simulated, this can be achieved by, e.g., inserting an equilibrated homogeneous configuration in the center of the free volume, followed by preferential test insertions and deletions in the affected region. In a supersaturated vapor, however, the density is usually so low that it is sufficient to leave a vacuum behind as suggested by McDonald<sup>23</sup>.

Establishing a steady state by continuously removing the largest nuclei is the purpose and the main advantage of McDonald's demon. Consequently, the further behavior of these nuclei cannot be tracked. It is assumed that most of the nuclei that are extracted would have continued to grow and that the demon intervention rate  $\mathcal{J}_\Theta$  is therefore similar to the actual nucleation rate  $\mathcal{J}$ . The deviation between these rates can also be quantified by regarding the size evolution of a single nucleus in terms of a discrete one-dimensional random walk over the order parameter  $\nu$ . At each size transition,  $\nu$  is either decreased or increased by one<sup>27</sup>. The short-term growth probability, corresponding to a size increase in the next step, is then given by

$$w = \left( 1 + \frac{\mathcal{Z}_{\nu-1}}{\mathcal{Z}_{\nu+1}} \right)^{-1}, \quad (9)$$

where  $\mathcal{Z}_{\nu\pm 1}$  is the grand canonical partition function under the condition that the nucleus contains  $\nu \pm 1$  particles. Neglecting all discrete size effects, the long-term growth probability  $q_\nu$ , which corresponds to the cases where the nucleus never evaporates completely and thus

eventually reaches arbitrarily large sizes, has the property<sup>27</sup>

$$\frac{d\mathcal{Z}}{\mathcal{Z}d\nu} = \frac{-d(dq_\nu/d\nu)}{2(dq_\nu/d\nu)d\nu}. \quad (10)$$

Using adequate boundary conditions, the long-term growth probability of the nuclei that are removed by the demon can be determined as

$$q_\Theta = \frac{\int_1^\Theta \mathcal{Z}_\nu^{-2} d\nu}{\int_1^\infty \mathcal{Z}_\nu^{-2} d\nu}. \quad (11)$$

The intervention rate is therefore related to the nucleation rate by

$$\mathcal{J}_\Theta \int_1^\Theta \exp\left(\frac{2\Delta\Omega_\nu}{k_B T}\right) d\nu = \mathcal{J} \int_1^\infty \exp\left(\frac{2\Delta\Omega_\nu}{k_B T}\right) d\nu. \quad (12)$$

In particular, for a threshold size sufficiently above  $\nu^*$  the approximation  $\mathcal{J} \approx \mathcal{J}_\Theta$  is valid<sup>27</sup>.

The truncated-shifted Lennard-Jones (tsLJ) fluid accurately describes the fluid phase coexistence of noble gases and methane<sup>10</sup>, avoiding long-range corrections which are tedious for inhomogeneous systems. Homogeneous vapor to liquid nucleation of the tsLJ fluid was studied here by GCMD simulation with McDonald's demon at temperatures of 0.65 to 0.95 in units of  $\varepsilon/k_B$  (where  $\varepsilon$  is the energy parameter of the Lennard-Jones potential). Note that the triple point temperature of the tsLJ fluid is  $T_3 = 0.65$  while  $T_c$  is 1.078 so that the entire relevant temperature range is covered<sup>10,17</sup>. The Stillinger<sup>28</sup> criterion was used to discern the emerging liquid from the surrounding supersaturated vapor and nuclei were determined as biconnected components.

### III. SIMULATION RESULTS

Figure 1 shows the aggregated number of demon interventions in one of the present GCMD simulations and, for comparison, the number of nuclei in a MD simulation of the canonical ensemble under similar conditions. The constant value of the supersaturation

$$S = \exp\left(\frac{\mu - \mu_\sigma(T)}{k_B T}\right), \quad (13)$$

in the GCMD simulation agreed approximately with the time-dependent  $S$  in the  $NVT$  simulation about  $t = 400$  after simulation onset in units of  $\sigma(m/\varepsilon)^{1/2}$ , wherein  $\sigma$  is the size parameter of the Lennard-Jones potential and  $m$  is the mass of a particle.

During the  $NVT$  run, however,  $S$  decreased from about 3 to 1.5. The observed rate of formation was significantly lower for larger nuclei, which is partly due to the depletion of the vapor over simulation time. Depletion causes less monomers to interact with a nucleus surface when large nuclei are formed because by that time, a substantial amount of particles already belong to the liquid. Moreover, a small nucleus will eventually decay with a higher probability, given by  $1-q$ , instead of growing to arbitrarily large sizes, cf. Eq. (11). Therefore, large nuclei are necessarily formed at a lower rate.

In Fig. 2, it can be seen how the decreasing supersaturation in the canonical ensemble MD simulation affects the nucleus size distribution. Around  $t = 400$ , the distribution of small nuclei present per volume was similar in both simulation approaches. Near and above the critical size, i.e., 27 particles according to CNT, cf. Tab. I, deviations arise because of the different boundary conditions. Comparing the distribution for the grand canonical steady state with the corresponding theoretical prediction shows that CNT underestimates the number of nuclei present in the metastable state, confirming the result of Talanquer<sup>2</sup> that CNT exaggerates the free energy of nucleus formation.

CNT is also known to underestimate the nucleation rate of unpolar fluids<sup>15</sup>. The determined demon intervention rates confirm this conclusion, cf. Tab. I, and as shown in Fig. 3, the HSL is significantly more accurate than CNT for low temperatures. For  $T = 0.85$ , HSL and CNT lead to similar predictions, deviating from simulation results by two orders of magnitude. At  $T = 0.95$ , a nucleation rate of  $\ln \mathcal{J} = -16.08$  was obtained for  $S = 1.146$  (using  $\Theta > 3 \nu_{\text{SPC}}^*$ ) where CNT predicts  $\ln \mathcal{J}_{\text{CNT}} = -19.99$ , cf. Tab. I, as opposed to  $\ln \mathcal{J}_{\text{HSL}} = -24.27$ . Thus, HSL breaks down at high temperatures for the tsLJ fluid. Present results generally agree with nucleation rates obtained by  $NVT$  simulation at temperatures between 0.65 and 0.95, as can be seen by comparison with the SPC modification that was correlated to data from canonical ensemble MD simulation<sup>15</sup>.

Figure 4 shows how the choice of  $\Theta$  affects the nucleus temperature. The largest nuclei allowed to remain in the system have a highly elevated temperature and the amount of nucleus overheating can be explained by considering the boundary condition that McDonald's demon imposes on size fluctuations. Only nuclei that do not fluctuate to sizes above  $\Theta$  remain in the system for a significant time. Almost all nuclei with  $\nu \approx \Theta$  approach the point where overheating due to the enthalpy of vaporization released during condensation counterbalances the supercooling of the vapor. Note that this effect is much stronger than the

overheating  $\Delta T^*$  of the critical nucleus according to CNT due to nucleation kinetics<sup>1</sup>

$$\Delta T^* = \frac{2f_Z k_B T^2}{\Delta h^v}, \quad (14)$$

where  $f_Z$  is the Zěl'dovič factor and  $\Delta h^v$  is the enthalpy of vaporization, evaluating to  $\Delta T_{\text{CNT}}^* = 0.00608$  in the present case.

With a threshold far below the critical size, the intervention rate of McDonald's demon is several orders of magnitude higher than the steady-state nucleation rate, cf. Tab. II and Fig. 5. In agreement with Eq. (12),  $\mathcal{J}_\Theta$  reaches a plateau for  $\Theta > \nu_{\text{SPC}}^*$ . In particular, the approximation  $\mathcal{J} \approx \mathcal{J}_\Theta$  is valid for all values shown in Tab. I and Fig. 3. As Tab. II also shows, the density and the pressure of the supersaturated vapor have very good convergence properties with respect to the intervention threshold size and can already be accurately obtained at a high accuracy for  $\Theta$  values near the critical size.

#### IV. CONCLUSION

GCMD with McDonald's demon was established as a method for steady-state simulation of nucleation processes. The main purpose of the new method consists in directly simulating a metastable state that undergoes a phase transition at a high rate without being limited to sampling only the short timespan until nucleation occurs.

By implication, growth or decay processes of very large nuclei are not covered. These have to be considered using the cutoff correction given by Eq. (12) unless the intervention threshold size is significantly larger than  $\nu^*$ . Due to an intervention scheme based on the single order parameter  $\nu$ , other relevant order parameters such as shape or temperature of the nuclei can experience a perturbation for a nucleus size similar to  $\Theta$ . It was shown for the nucleus temperature that this only concerns the largest nuclei in the system and that the range of nucleus sizes unaffected by intervention based overheating can be extended arbitrarily if a sufficiently high value of  $\Theta$  is chosen.

The intervention rate necessarily approaches the nucleation rate for increasing values of the intervention threshold size. The dependence of  $\mathcal{J}_\Theta$  on  $\Theta$  is already accurately described for  $\Theta > \nu^*/2$  by modeling the nucleus size evolution as a one-dimensional random walk without taking any other order parameter into account.

For vapor to liquid nucleation of the tsLJ fluid, a series of simulations was conducted over

a wide range of temperatures. Good agreement with canonical ensemble MD simulation results was reached. It was confirmed that CNT overstates the free energy of nucleus formation and underpredicts the nucleation rate. HSL accurately describes nucleation near the triple point temperature; at high temperatures, however, significant deviations are present.

**Acknowledgment.** The authors would like to thank Martin Bernreuther (Stuttgart), Guram Chkonia (Cologne), Hans Hasse (Kaiserslautern), Svetlana Miroshnichenko (Paderborn), Srikanth Sastry (Bangalore), Chantal Valeriani (Edinburgh), and Jan Wedekind (Barcelona) for openly discussing methodological issues as well as Deutsche Forschungsgemeinschaft (DFG) for funding the collaborative research center (SFB) 716 at Universität Stuttgart. The presented research was conducted under the auspices of the Boltzmann-Zuse Society of Computational Molecular Engineering (BZS), and the simulations were performed on the HP XC4000 supercomputer at the Steinbuch Centre for Computing, Karlsruhe, under the grant LAMO.

- 
- <sup>1</sup> J. Feder, K. C. Russell, J. Lothe, and G. M. Pound, *Adv. Phys.* **15**, 111 (1966).
  - <sup>2</sup> V. Talanquer, *J. Phys. Chem. B* **111**, 3438 (2007).
  - <sup>3</sup> J. Vrabec, M. Horsch, and H. Hasse, *J. Heat Transfer* **131**, 043202 (2009).
  - <sup>4</sup> P. G. Debenedetti, *Nature* **441**, 168 (2006).
  - <sup>5</sup> A. C. Pan, T. J. Rappl, D. Chandler, and N. P. Balsara, *J. Phys. Chem. B* **110**, 3692 (2006).
  - <sup>6</sup> D. W. Oxtoby and R. Evans, *J. Chem. Phys.* **89**, 7521 (1988).
  - <sup>7</sup> X. C. Zeng and D. W. Oxtoby, *J. Chem. Phys.* **94**, 4472 (1991).
  - <sup>8</sup> T. V. Bykov and A. K. Shchekin, *Colloid J.* **61**, 144 (1999).
  - <sup>9</sup> M. J. Uline and D. S. Corti, *J. Chem. Phys.* **129**, 234507 (2008).
  - <sup>10</sup> J. Vrabec, G. K. Kedia, G. Fuchs, and H. Hasse, *Mol. Phys.* **104**, 1509 (2006).
  - <sup>11</sup> R. Hołyst and M. Litniewski, *Phys. Rev. Lett.* **100**, 055701 (2008).
  - <sup>12</sup> M. Schrader, P. Virnau, and K. Binder, *Phys. Rev. E* **79**, 061104 (2009).
  - <sup>13</sup> A. V. Neimark and A. Vishnyakov, *J. Phys. Chem. B* **109**, 5962 (2005).
  - <sup>14</sup> K. Yasuoka and M. Matsumoto, *J. Chem. Phys.* **109**, 8451 (1998).
  - <sup>15</sup> M. Horsch, J. Vrabec, and H. Hasse, *Phys. Rev. E* **78**, 011603 (2008).

- <sup>16</sup> L. M. Ghiringhelli, C. Valeriani, J. H. Los, E. J. Meijer, A. Fasolino, and D. Frenkel, *Mol. Phys.* **106**, 2011 (2008).
- <sup>17</sup> J. A. van Meel, A. J. Page, R. P. Sear, and D. Frenkel, *J. Chem. Phys.* **129**, 204505 (2008).
- <sup>18</sup> R. C. Tolman, *J. Chem. Phys.* **17**, 333 (1949).
- <sup>19</sup> B. N. Hale, *Phys. Rev. A* **33**, 4156 (1986).
- <sup>20</sup> J. Wedekind, R. Strey, and D. Reguera, *J. Chem. Phys.* **126**, 134103 (2007).
- <sup>21</sup> G. Chkonia, J. Wölk, R. Strey, J. Wedekind, and D. Reguera, *J. Chem. Phys.* **130**, 064505 (2009).
- <sup>22</sup> M. M. Cielinski, M. Sc. thesis, University of Maine (1985).
- <sup>23</sup> J. E. McDonald, *Am. J. Phys.* **31**, 31 (1962).
- <sup>24</sup> M. Lupkowski and F. van Swol, *J. Chem. Phys.* **95**, 1995 (1991).
- <sup>25</sup> M. P. Allen and D. J. Tildesley, *Computer Simulation of Liquids* (Clarendon, Oxford, 1987).
- <sup>26</sup> J. W. P. Schmelzer, G. Röpke, and F.-P. Ludwig, *Phys. Rev. C* **55**, 1917 (1997).
- <sup>27</sup> M. Horsch, S. Miroshnichenko, and J. Vrabec, *J. Stat. Phys.* (2009), L'viv (Львів), to appear.
- <sup>28</sup> F. H. Stillinger, *J. Chem. Phys.* **38**, 1486 (1963).

Table I:

Average number of particles and intervention rate of McDonald's demon during GCMD simulation as well as the nucleation rate approximated by  $\mathcal{J} \approx q_\Theta(\text{CNT})\mathcal{J}_\Theta$ , cf. Eqs. (11) and (12), in dependence of simulation conditions, i.e., temperature (in units of  $\varepsilon/k_B$ ), supersaturation, intervention threshold size (in particles), and system volume (in units of  $\sigma^3$ ), compared to theoretical predictions for the nucleation rate according to CNT and the SPC modification; all logarithms are given with respect to the reduced rates, normalized by  $(m/\varepsilon)^{1/2}\sigma^{-4}$ . Note that the intervention threshold size is sufficiently larger than the critical size in all cases.

$T$	$S$	$\Theta$	$V$	$N$	$\ln \mathcal{J}_\Theta$	$\ln \mathcal{J}$	$\ln \mathcal{J}_{\text{CNT}}$	$\ln \mathcal{J}_{\text{SPC}}$	$\nu_{\text{CNT}}^*$	$\nu_{\text{SPC}}^*$
0.65	3.500	66	$1.38 \times 10^7$	261 000	-21.12	-21.12	-25.80	-20.83	30	27
	3.800	45	$2.40 \times 10^7$	529 000	-18.42	-18.42	-23.44	-18.86	24	21
	4.100	36	$2.03 \times 10^7$	517 000	-16.29	-16.33	-21.60	-17.44	21	17
	4.400	30	$1.54 \times 10^7$	487 000	-13.79	-13.80	-19.96	-16.20	18	14
0.7	2.496	74	$2.16 \times 10^7$	518 000	-22.08	-22.08	-26.40	-21.33	41	39
	2.616	75	$3.95 \times 10^7$	1 040 000	-20.63	-20.63	-24.50	-19.70	36	32
	2.692	72	$1.85 \times 10^7$	518 000	-19.04	-19.04	-23.48	-18.83	33	29
	2.774	60	$3.51 \times 10^7$	1 030 000	-18.24	-18.24	-22.49	-18.06	30	26
	2.866	51	$2.02 \times 10^6$	63 800	-16.77	-16.77	-21.49	-17.30	27	23
	2.959	45	$1.50 \times 10^7$	513 000	-15.65	-15.65	-20.59	-16.62	25	21
0.85	1.426	219	$1.68 \times 10^7$	1 040 000	-19.62	-19.62	-22.28	-18.66	80	80
	1.440	198	$1.62 \times 10^7$	1 030 000	-17.89	-17.89	-21.51	-17.98	74	72
	1.461	186	$1.87 \times 10^6$	125 000	-16.55	-16.55	-20.48	-17.10	66	62
	1.483	144	$6.24 \times 10^6$	431 000	-15.54	-15.54	-19.41	-16.20	58	54
0.9	1.240	209	$3.45 \times 10^6$	256 000	-21.33	-21.35	-23.24	-20.33	137	149
	1.260	162	$3.23 \times 10^6$	255 000	-18.21	-18.26	-21.29	-18.37	110	116
	1.280	127	$2.98 \times 10^6$	247 000	-17.01	-17.10	-19.72	-16.91	90	91
0.95	1.146	564	$4.88 \times 10^6$	516 000	-16.08	-16.08	-19.99	-17.89	156	175

Table II:

Pressure supersaturation  $p/p_\sigma(T)$  and density supersaturation  $\rho/\rho_\sigma(T)$  as well as the intervention rate of McDonald's demon in dependence of simulation conditions along with the long-term growth probability  $q_\Theta$  of a nucleus containing  $\Theta$  particles, cf. Eq. (11), according to CNT.

$T$	$S$	$\Theta$	$V$	$p/p_\sigma(T)$	$\rho/\rho_\sigma(T)$	$\ln \mathcal{J}_\Theta$	$q_\Theta(\text{CNT})$
0.7	2.496	10	$5.38 \times 10^6$	2.70	3.16	-13.55	$3.98 \times 10^{-7}$
		15	$4.31 \times 10^7$	2.69	3.17	-15.65	$4.61 \times 10^{-5}$
		20	$4.31 \times 10^7$	2.75	3.26	-16.99	$1.25 \times 10^{-3}$
		25	$5.38 \times 10^6$	2.78	3.32	-17.63	0.01
		30	$2.16 \times 10^7$	2.77	3.31	-19.20	0.07
		35	$5.38 \times 10^6$	2.78	3.32	-19.89	0.20
		48	$4.31 \times 10^7$	2.78	3.33	-21.74	0.77
		56	$2.16 \times 10^7$	2.78	3.32	-21.18	0.95
		65	$4.31 \times 10^7$	2.78	3.32	-21.90	>0.99
		74	$2.16 \times 10^7$	2.77	3.32	-22.08	>0.99
0.9	1.240	89	$3.45 \times 10^6$	1.33	1.67	-18.87	0.04
		149	$3.45 \times 10^6$	1.34	1.69	-19.80	0.62
		209	$3.45 \times 10^6$	1.34	1.68	-21.33	0.98
0.9	1.260	70	$3.23 \times 10^6$	1.36	1.74	-16.64	0.04
		116	$3.23 \times 10^6$	1.37	1.78	-17.82	0.55
		162	$3.23 \times 10^6$	1.37	1.79	-18.21	0.95
0.9	1.280	55	$2.98 \times 10^6$	1.37	1.77	-15.69	0.04
		91	$2.98 \times 10^6$	1.39	1.87	-16.08	0.47
		127	$2.98 \times 10^6$	1.39	1.88	-17.01	0.91

**Figure 1** Top: number per unit volume  $\rho_n$  of nuclei containing  $\nu > 25$  ( $\cdot \cdot -$ ), 50 ( $-$ ), and 150 ( $- -$ ) particles in a *NVT* simulation at  $T = 0.7$  and  $\rho = 0.004044$  (in units of  $\sigma^{-3}$ ) as well as the aggregated number of McDonald’s demon interventions per unit volume in a GCMD simulation with  $T = 0.7$ ,  $S = 2.8658$ , and  $\Theta = 51$  ( $\cdot \cdot \cdot$ ) over simulation time; bottom: pressure over simulation time for the *NVT* simulation ( $- -$ ) and the GCMD simulation ( $-$ ).

**Figure 2** Nucleus number per unit volume  $\rho_n$  over nucleus size  $\nu$  from *NVT* simulation at  $T = 0.7$  and  $\rho = 0.004044$ , with sampling intervals of  $320 \leq t \leq 480$  ( $\circ$ ) and  $970 \leq t \leq 1130$  ( $\diamond$ ) after simulation onset, and from GCMD simulation with  $T = 0.7$ ,  $S = 2.8658$ , and  $\Theta = 51$  ( $\bullet$ ) in comparison with a prediction for the same conditions based on CNT ( $-$ ).

**Figure 3** Nucleation rate logarithm  $\ln \mathcal{J}$  over supersaturation  $S$  at  $T = 0.65, 0.7,$  and  $0.85$  according to CNT ( $-$ ), the SPC modification ( $- -$ ) as well as HSL ( $\cdot \cdot \cdot$ ) compared to present GCMD simulation results ( $\circ$ ).

**Figure 4** Nucleus temperature over nucleus size from GCMD simulation at  $T = 0.7$  and  $S = 2.4958$  for an intervention threshold size of  $\Theta = 15$  ( $\blacktriangle$ ), 30 ( $\circ$ ), 48 ( $\bullet$ ), 65 ( $\nabla$ ), and 74 particles ( $\blacksquare$ ); dotted line: saturation temperature  $T_\sigma = 0.7965$  of the vapor at constant pressure  $p = 0.134$ , which corresponds to the chosen supersaturation; dashed lines: guide to the eye.

**Figure 5** Intervention rate logarithm  $\ln \mathcal{J}_\Theta$  over intervention threshold size  $\Theta$  of McDonald’s demon during GCMD simulation at  $T = 0.7$  and  $S = 2.4958$  ( $\square$ ) in comparison with predictions based on CNT ( $-$ ) and the SPC modification ( $- -$ ); dotted line: CNT prediction shifted to the actual value of the nucleation rate; vertical line: critical size according to the SPC modification.

Figure 1:

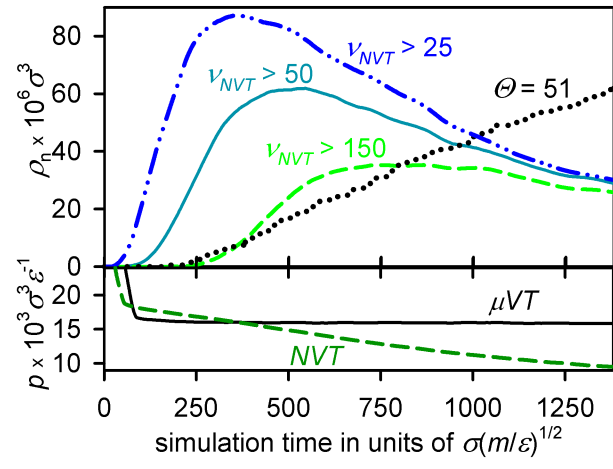


Figure 2:

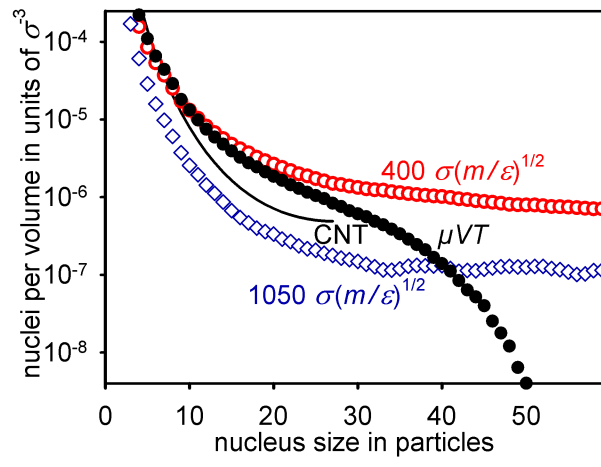


Figure 3:

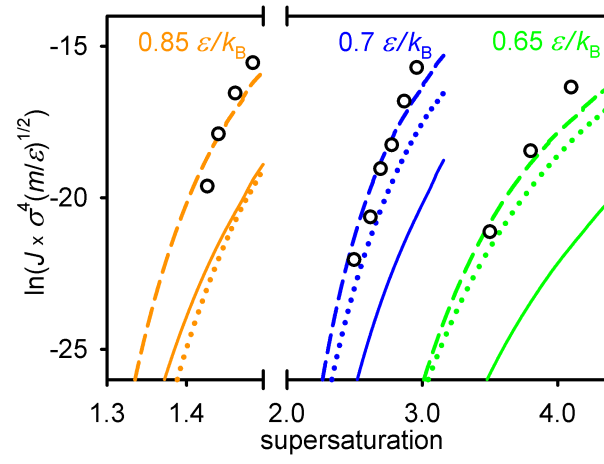


Figure 4:

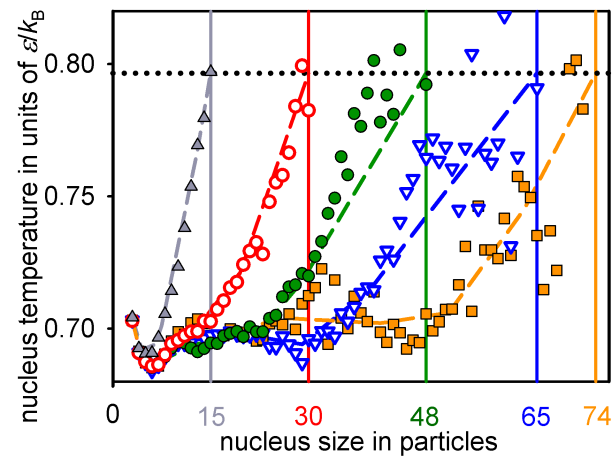


Figure 5:

